Localised to intraligand charge-transfer states in cyclometalated platinum complexes: an experimental and theoretical study into the influence of electron-rich pendants and modulation of excited states by ion binding†

David L. Rochester,[a] Stéphanie Develay,[a] Stanislav Záliš*[b] and J. A. Gareth Williams*[a]

Received 18th September 2008, Accepted 14th November 2008
First published as an Advance Article on the web 26th January 2009
DOI: 10.1039/b816375h

The neopentyl ester of 1,3-di(2-pyridyl)benzene-5-boronic acid (dpy-B) is a useful intermediate in the divergent synthesis of N^C^N-coordinating, 1,3-di(2-pyridyl)benzene ligands, HL^n, that carry aryl substituents at the 5-position of the central ring. The platinum(II) complexes, PtL^nCl, of several such ligands have been prepared, incorporating pendant anisoles, arylamines, an oxacrown, and an azacrown, all of which are strongly luminescent in solution at 298 K. The emission of the complexes is partially quenched by oxygen, and all of the compounds are very efficient sensitisers of singlet oxygen. The quantum yields of $^1O_2$ formation have been measured on the basis of the intensity of the O_2 $^1\Delta_g$ emission at 1270 nm, and are in the range 0.25–0.65. Density functional theory (DFT) calculations have been carried out that include the effect of the solvent, on the unsubstituted complex PtL^1Cl and on the derivatives incorporating *p*-dimethylaminophenyl and phenyl-15-mono-*N*-azacrown-5 pendants (PtL^9Cl and $PtL^{12}Cl$ respectively). Absorption spectra have been simulated on the basis of the calculated singlet excitations: they closely resemble the experimental spectra. In particular, the DFT successfully accounts for the appearance of low-energy absorption bands that accompany the introduction of the aryl pendants, indicating the participation of the aryl group in the HOMO but not significantly in the LUMO. The calculated lowest energy triplet excitation of PtL^1Cl is close to the observed 0–0 emission maximum of this complex in solution. Taking together data for this series of complexes and related compounds previously studied, the energies of the lowest-energy spin-allowed absorption bands are shown to correlate approximately linearly with the oxidation peak potential. The emission energies show a similar correlation in toluene, but in CH_2Cl_2 the value for PtL^9Cl is anomalously low. The differing emission properties of this complex in the two solvents suggest a switch to a TICT-like state in CH_2Cl_2 (TICT = twisted intramolecular charge transfer), stabilised in the more polar environment. Transient DC photoconductivity measurements confirm that the dipole moment of the triplet excited state is larger in CH_2Cl_2 than in toluene. The azacrown $PtL^{12}Cl$ displays similar behaviour. Binding of metal ions such as Ca^{2+} to the azacrown unit of this complex leads to a pronounced blue shift in the emission, which can be readily understood in terms of the large increase in the TICT energy that will accompany the binding of the metal ion to the lone pair of the azacrown nitrogen atom.

Introduction

Transition metal complexes that emit efficiently from triplet excited states are the subject of a great deal of current research interest. Apart from the insight into fundamental excited state processes that they offer, there are numerous applications of such compounds. For example, the new generation of display screen technology–organic light-emitting devices (OLEDs)–can benefit from the incorporation of such materials to induce emission from otherwise wasted triplet states.[1–3] Meanwhile, triplet excited states of transition metal complexes may be sufficiently long-lived to allow time for useful chemical processes to occur following absorption of light, such as energy and electron transfer, central to the field of light-to-chemical energy conversion.[4] Long lifetimes under ambient conditions can also be exploited in sensor technology, not only offering a means of discriminating from short-lived background emission, but also allowing lifetimes to be used as a reporter parameter, in contrast to the normally used methods based on intensity or wavelength.[5,6] The design of triplet emitters that respond to their environment or to the presence of analytes of interest through modulation of the lifetime and/or emission profile is key to the development of such sensors.[7]

As far as platinum(II) complexes of polyimine ligands are concerned, the number of compounds that emit efficiently in solution at room temperature has increased greatly over the past decade.[8] The use of cyclometalating ligands, or co-ligands such as acetylides, has proved to be a particularly successful strategy for promoting luminescence: the strong ligand-field associated with such ligands ensures that the severely distorted metal-centred (d–d) states—population of which is responsible for non-radiative

[a]*Department of Chemistry, University of Durham, Durham, U.K. DH1 3LE. E-mail: j.a.g.williams@durham.ac.uk*
[b]*J. Heyrovsky Institute of Physical Chemistry, Dolejskova 3, 182 23 Prague 8, Czech Republic. E-mail: stanislav.zalis@jh-inst.cas.cz*

† Electronic supplementary information (ESI) available: Additional synthetic details; Fig. S1–S7; Tables S1 and S2. See DOI: 10.1039/b816375h

decay of simple Pt complexes such as Pt(bpy)Cl_2—are displaced to high energies.[8,9] A number of studies during the past decade have reported on luminescent platinum-based sensory systems.[10] Some of these make use of binding moieties such as crown ethers and related ligands, appended onto the core of emissive complexes.[11] Binding of the analyte modulates the properties of the excited states, its influence being manifest through a change in the emission characteristics, typically the intensity.

We have been exploring the chemistry of platinum(II) complexes with terdentate cyclometalating ligands based on 1,3-di(2-pyridyl)benzene (HL^1), which offer the metal ion an N^C^N coordination environment (Chart 1).[12,13] These compounds are amongst the brightest Pt-based emitters in solution at room temperature; *e.g.* for the parent complex, [PtL^1Cl], $\Phi_{lum} = 0.60$ and $\tau = 7.2$ μs in deoxygenated dichloromethane.[12] The complexes are thermally stable and sublimable, rendering them appropriate for incorporation into OLEDs: high device efficiencies have been obtained in this way,[14,15] including near-IR and white light emitting devices that exploit excimer or aggregate emission.[16,17] In earlier work, we found that the introduction of a range of simple aryl substituents into the central 4-position of the N^C^N ligand (Chart 1) allowed the emission energy E_{em} to be tuned over a range of ~3500 cm^{-1}.[13] E_{em} decreased in the order R = H > mesityl > 2-pyridyl > 4-tolyl > 4-biphenylyl > 2-thienyl, in line with the increasing electron richness (= decreasing oxidation potential) of the complex. However, for the derivative incorporating a *p*-dimethylaminophenyl substituent, PtL^9Cl, the emission energy was substantially lower than that anticipated on this basis. We tentatively attributed this, and other differences from the other complexes (*vide infra*), to the introduction of an emissive triplet intraligand charge transfer (^{3}ILCT) state.[13] In this contribution, we probe in more detail the nature of the excited state of PtL^9Cl through a combination of experimental and theoretical methods. We report the synthesis and luminescence properties of a range of new complexes incorporating other electron-rich substituents, including phenols, amines, oxacrown and azacrown ethers (Chart 2), and explore the balance between charge-transfer and ligand-localised emission in such systems.

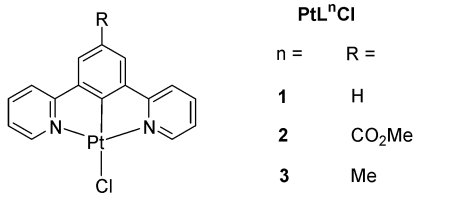

PtL^{n}Cl			
n =	R =		
1	H		
2	CO_2Me		
3	Me		
4	2-pyridyl	7	4-tolyl
5	mesityl	8	2-thienyl
6	4-biphenylyl	9	4-(dimethylamino)phenyl

Chart 1 Structures of the complexes investigated in the previous study.[12,13]

Results and discussion

1. Synthesis of new aryl-appended, N^C^N-coordinating ligands and their Pt(II) complexes

The new ligands HL^{10-15} were prepared by one or other of two closely related methods, as shown in Scheme 1. Previously, we found that Suzuki cross-coupling reactions of aryl boronic acids with the key intermediate 1,3-di(2-pyridyl)-5-bromobenzene (dpyb-Br) provide a convenient, divergent route to aryl-substituted N^C^N ligands HL^n. For example, ligands HL^5 and HL^6 were prepared in this way from mesitylboronic acid and 4,4′-biphenyl-1-boronic acid respectively. In the current work, this method was employed to prepare ligands HL^9, HL^{13} and HL^{14}.

A potentially more versatile strategy would be to make use of the reverse coupling, in which the boronic acid unit is incorporated into the dipyridylbenzene, thus generating a versatile intermediate for coupling with a wider range of aryl halides. The new intermediate dpyb-B, the neopentylglycolate ester of 1,3-di(2-pyridyl)benzene-5-boronic acid (Scheme 1), was prepared readily by a Miyaura cross-coupling reaction[18] between dpyb-Br and bis(neopentyl)glycolato diboron (B_2neo_2), catalysed by Pd(dppf)Cl_2 in the presence of potassium acetate. The strategy

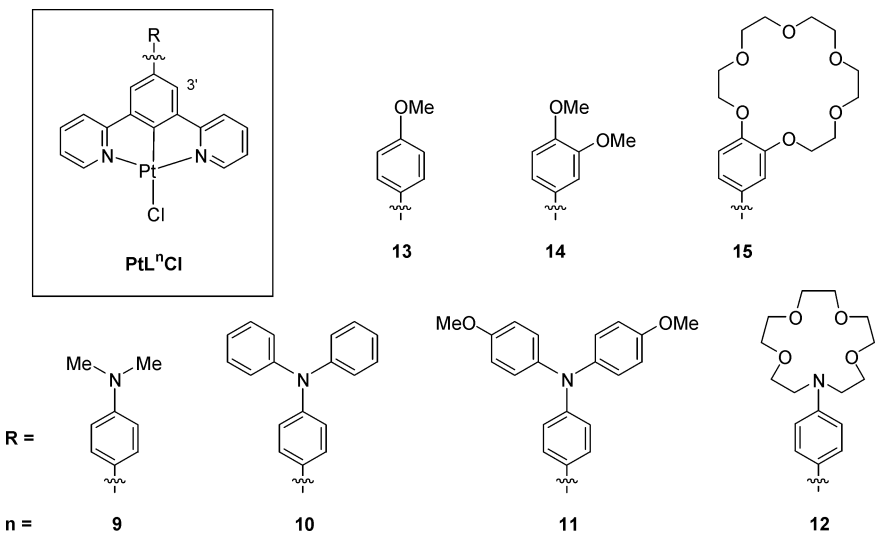

Chart 2 Structures of the new complexes described here.

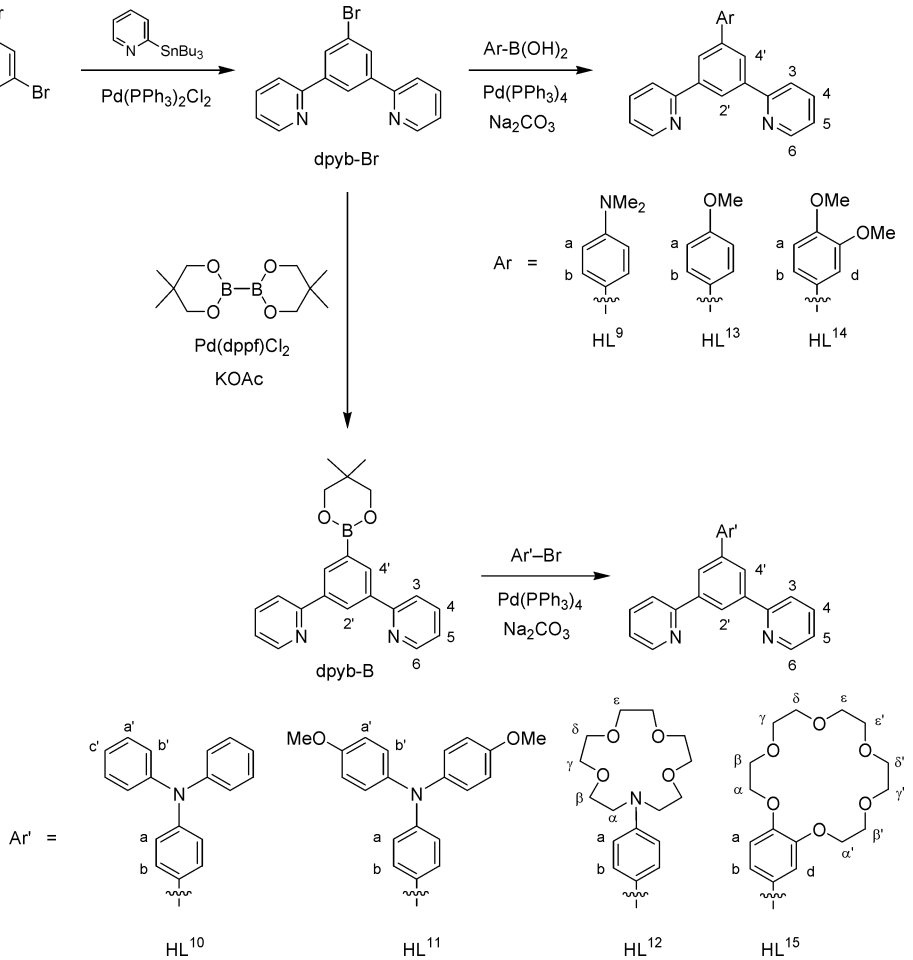

Scheme 1 Synthetic routes to the new ligands.

is directly analogous to that developed previously in our laboratory for the boronic acid derivatives of terpyridine and 4′-phenylterpyridine, which serve as versatile intermediates in the preparation of substituted terpyridines.[19] The subsequent cross-coupling reaction of dpyb-B with 4-bromo-N,N-diphenylaniline proceeded readily under standard conditions to generate HL^{10}. The method was readily extrapolated to the *p*-methoxy-substituted analogue, HL^{11}, and to the azacrown- and oxacrown-appended ligands HL^{12} and HL^{15}. The requisite 4-bromophenyl-*N*-monoaza-15-crown-5 for the synthesis of HL^{12} was prepared by standard cyclisation methods (see ESI†).

The platinum(II) complexes of the ligands were obtained upon reaction with K_2PtCl_4, using either acetic acid or a mixture of acetonitrile and water as the solvent. Typical reaction times were 2–3 days at reflux; further details for individual complexes are provided in the Experimental. Crystals of $PtL^{10}Cl$ and $PtL^{12}Cl$ suitable for X-ray diffraction analysis were obtained from solutions in CH_2Cl_2. Unfortunately, disorder hampered a full refinement, but the data was more than adequate to confirm the identity of the complexes (see Fig. S6 and S7 in the ESI†).

2. Density functional theory (DFT) calculations of PtL^1Cl

Based upon the highly structured profile of the emission spectrum, and the very small Stokes shift between the highest energy emission band and the weak but distinct $S_0 \rightarrow T_1$ absorption band, we previously assigned the emission from this complex to a state of predominant π–π* character, in which some contribution from the metal nevertheless promotes the triplet radiative decay constant.[12] Such an interpretation is supported by the DFT calculations of Sotoyama *et al.*, who modelled the parent PtL^1Cl and methyl derivative PtL^3Cl in the gas phase.[20] In the present work, time-dependent density functional theory (TD-DFT) calculations have been carried out to explore the nature of the excited states, taking into account the influence of the solvent. These procedures have been applied to investigate the profound differences observed between PtL^1Cl and the amino-substituted complex PtL^9Cl. Calculations were performed using B3LYP or PBE0 functionals together with CPCM solvent description with CH_2Cl_2 as the solvent.

Initially, ground-state DFT geometry optimisation calculations were attempted in order to assess the reliability of the method: calculated results were compared to those obtained experimentally by X-ray crystallography for two of the complexes for which diffraction data is available (PtL^3Cl and PtL^6Cl).[13] Table S1 in the ESI† reveals the excellent agreement between calculated and experimental data.

TD-DFT was then applied to the parent unsubstituted complex PtL^1Cl at its energy-minimised geometry, in order to identify the main orbital components of the singlet transitions, together with

Table 1 TD-DFT B3LYP/CPCM (CH_2Cl_2) singlet excitation energies (eV) for [PtL^1Cl] with oscillator strength larger than 0.001, and corresponding experimental values

State	Main components (%)	Transition energy[a]/eV (nm)	Oscillator Strength	Expt. band max./nm	Extinction coefficient ε/M^{-1} cm^{-1}
a^3A	75 (HOMO → LUMO)	2.64 (471)	—	485	240
b^3A	90 (HOMO → LUMO + 1)	2.82 (440)	—	454	270
a^1A	92 (HOMO → LUMO)	3.20 (387)	0.004	—	—
b^1A	92 (HOMO → LUMO + 1)	3.25 (382)	0.155	401	7010
c^1A	97 (HOMO – 2 → LUMO)	3.62 (343)	0.011	380	8690
d^1A	91 (HOMO – 1 → LUMO)	3.62 (342)	0.005	—	—
g^1A	67 (HOMO – 1 → LUMO + 1)	3.96 (313)	0.081	332	6510
i^1A	78 (HOMO – 4 → LUMO) ($\pi\rightarrow\pi^*$) ligand	4.19 (296)	0.355	290	22200

[a] Corresponding wavelength (nm) in parenthesis.

their energies and oscillator strengths. The data are summarised in Table 1 and pertinent frontier orbitals are illustrated in Fig. 1(a). The results aid in the interpretation of a number of experimental observations. The lowest energy spin-allowed transitions in absorption, around 380–400 nm, can be attributed to the HOMO → LUMO and HOMO → LUMO + 1 transitions. An absorption spectrum has been simulated based on the excitation energies and their oscillator strengths, which matches closely the experimental spectrum (Fig. 2). Similarly, the lowest-energy *triplet* state is seen to be comprised predominantly of HOMO → LUMO character (Table 1), and the calculated energy is remarkably close to that of the 0–0 band found in the experimental spectrum (2.64 and 2.53 eV respectively). Some further comments and caveats on the assignment of bands in the spectrum by DFT are provided in the ESI†. For both singlet and triplet, the net charge distribution that accompanies the formation of the excited state is principally "outwards" from Pt/Cl/phenyl to the pyridine rings

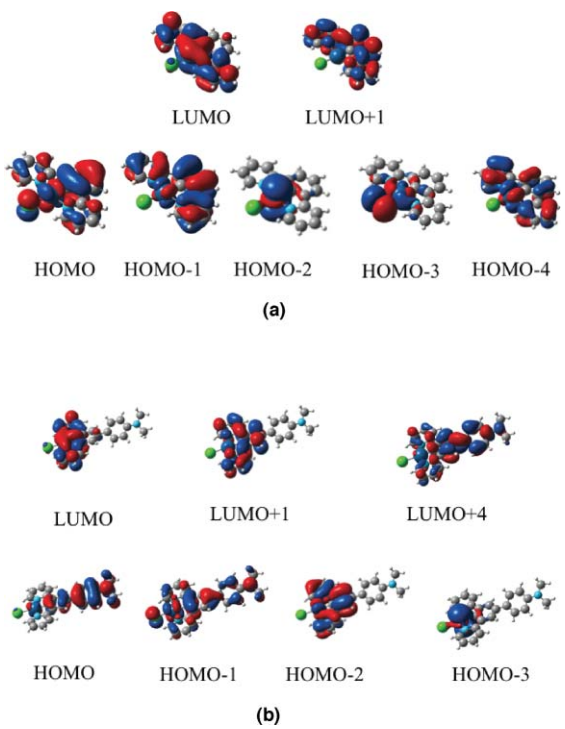

Fig. 1 Frontier orbitals of (a) PtL^1Cl, and (b) PtL^9Cl, calculated by DFT and including CH_2Cl_2 as the solvent.

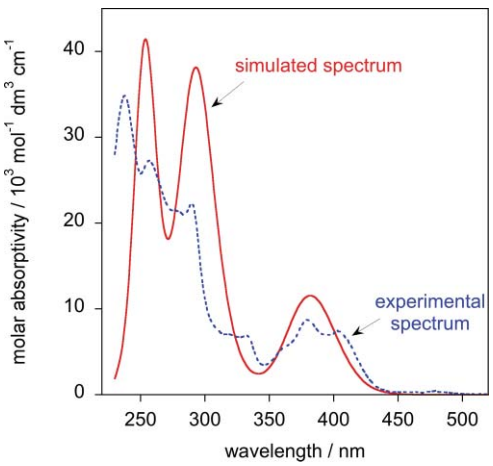

Fig. 2 Calculated absorption spectrum of [PtL^1Cl] (red solid line) in CH_2Cl_2 at 298 K, simulated using the TD-DFT data of Tables 2 and 3; also shown is the experimental spectrum under the same conditions (blue dashed line).

(Fig. 1a), in such a way that there will be little change in the dipole moment, as is clear from the calculated dipole differences for the excitations listed in Table 2. This would account for the relatively weak solvatochromism observed for this complex (e.g. a difference of only 300 cm^{-1} between the emission maxima in toluene and acetonitrile, representing the extremes of polarity for solvents in which the complex is soluble).

3. DFT calculations of PtL^9Cl: trends in absorption spectra

The 4-(dimethylamino)phenyl-substituted complex PtL^9Cl is bright orange as opposed to the yellow colour of the parent complex PtL^1Cl. This is due to a strong, broad absorption in the visible region, $\lambda_{max} = 431$ nm, $\varepsilon = 8880$ in CH_2Cl_2 at 298 K (Fig. 3). Previously we postulated that the emergence of this band might be due to a significant participation of the pendant aminophenyl group in the HOMO.[13] We now demonstrate that DFT calculations of PtL^9Cl, modelled in the presence of CH_2Cl_2 as the solvent, unequivocally support this hypothesis. The frontier orbitals of PtL^9Cl, calculated by DFT using B3LYP/CPCM, are shown in Fig. 1(b). The excitation energies of singlet transitions with oscillator strengths greater than 0.001 are listed in Table S2 in the ESI†. Table 2 compares the energies of the lowest-lying transitions of PtL^9Cl with those of PtL^1Cl, together with

Table 2 TD-DFT B3LYP/CPCM (CH_2Cl_2) lowest lying singlet and triplet excitation energies (eV) and the dipole moment differences between excited and ground state, calculated for [PtL^{1}L], [PtL^{9}L] and [PtL^{12}L]

	State	Main components (%)	Transition energy[a]/eV (nm)	Oscillator strength	$\Delta\mu/D$
[PtL^{1}L]	a^3A (T_1)	75 (HOMO → LUMO)	2.64 (471)	—	0.94
	b^3A (T_2)	90 (HOMO → LUMO + 1)	2.82 (440)	—	2.35
	a^1A (S_1)	92 (HOMO → LUMO)	3.20 (387)	0.004	1.10
	b^1A (S_2)	92 (HOMO → LUMO + 1)	3.25 (382)	0.155	3.99
[PtL^{9}L]	a^3A (T_1)	77 (HOMO → LUMO)	2.36 (525)	—	13.80
	b^3A (T_2)	93 (HOMO → LUMO + 1)	2.39 (518)	—	15.95
	a^1A (S_1)	95 (HOMO → LUMO)	2.65 (467)	0.041	26.89
	b^1A (S_2)	95 (HOMO → LUMO + 1)	2.65 (466)	0.042	22.61
[PtL^{12}L]	a^3A (T_1)	90 (HOMO → LUMO)	2.33 (531)	—	16.23
	b^3A (T_2)	78 (HOMO → LUMO + 1)	2.35 (526)	—	16.09
	a^1A (S_1)	97 (HOMO → LUMO)	2.58 (480)	0.040	23.21
	b^1A (S_2)	97 (HOMO → LUMO + 1)	2.60 (477)	0.039	27.52

[a] Corresponding wavelength (nm) in parenthesis.

the dipole moment differences between excited and ground states. The HOMO in PtL^{9}Cl is localised primarily on the pendent 4-dimethylaminophenyl group, rather than on the Pt-N^C^N unit as it is in PtL^{1}Cl. On the other hand, the closely lying LUMO and LUMO + 1 remain localised on the Pt-N^C^N moiety. Thus, the lowest-energy, HOMO → LUMO and HOMO → LUMO + 1 transitions have clear-cut intraligand charge transfer character. The simulated spectrum based on these data shown in Fig. 3 qualitatively describes the experimental spectrum: the marked difference between the spectra of PtL^{9}Cl and PtL^{1}Cl corresponds closely to what is observed in practice (Fig. 3 *versus* Fig. 2). The new HOMO → LUMO transition gives rise to a low-energy band that has no counterpart in PtL^{1}Cl, with a predicted wavelength of 467 nm (experimental value 431 nm).

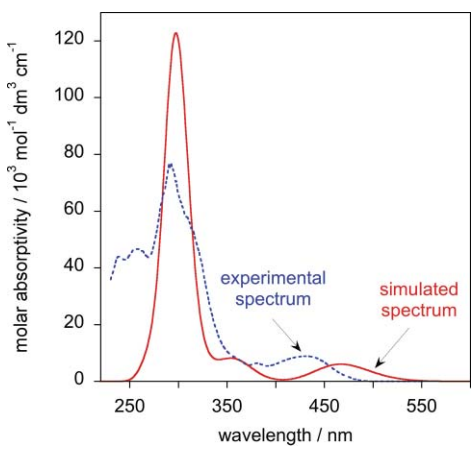

Fig. 3 Calculated absorption spectrum of [PtL^{9}Cl] (red solid line) in CH_2Cl_2 at 298 K, simulated using the TD-DFT data of Tables 3 and S1†; also shown is the experimental spectrum under the same conditions (blue dashed line).

The new aryl-substituted complexes prepared in this study, together with those from the previous work, have absorption maxima between the values of PtL^{1}Cl and PtL^{9}Cl (Table 3), reflecting the progressively increasing contribution of the aryl pendant to the HOMO as the pendant becomes more electron rich. A remarkably linear correlation is observed between the energy of the lowest-energy, spin-allowed intense absorption band

Table 3 Ground state UV-visible absorption data of the new platinum complexes in CH_2Cl_2 at 298 K, with data for PtL^{1}Cl and PtL^{9}Cl for comparison

Complex and substituent	Absorbance[a] λ_{max}/nm (ε/M^{-1}cm^{-1})
PtL^{1}Cl[b] H–	380 (8690), 401 (7010), 454 (270), 485 (240)
PtL^{9}Cl[c] Me_2N-C_6H_4–	380 (6410), 431 (8880)
PtL^{10}Cl Ph_2N-C_6H_4–	380 sh (7200), 422 (7160), 495 (110)
PtL^{11}Cl (p-MeO-C_6H_4)$_2$N-C_6H_4–	423 (7400), 498 (100)
PtL^{12}Cl azacrown	360 (7260), 379 (6100), 432 (8010)
PtL^{13}Cl MeO-C_6H_4–	364 (4070), 381 (6300), 420 (7200), 497 (120)
PtL^{14}Cl $(MeO)_2$-C_6H_3–	362 (3670), 381 (6200), 422 (6970), 497 (100)
PtL^{15}Cl oxacrown	363 (3380), 381 (5930), 420 (6400), 498 (120)

[a] For bands > 350 nm. [b] Data from reference 12. [c] Data from reference 13.

(E_{abs}) and the oxidation potential E_p^{ox} for the collective set of complexes (Fig. 4). That the energy depends on the oxidation potential alone, the reduction potential seemingly irrelevant, can be readily rationalised from the DFT results. Inspection of the frontier orbitals of PtL^{1}Cl in Fig. 1a reveals that the 4-position of the phenyl ring makes a major contribution to the HOMO but only a minor contribution to the LUMO and is a node in LUMO + 1. Thus, the HOMO (and hence oxidation) should be significantly affected by the substituent, whereas the LUMO (hence reduction potential) and LUMO + 1 will be much less so. The observed red shifts with increasing electron-donating ability of substituent thus reflect an increase in the HOMO level and a LUMO that remains essentially unchanged.

4. Luminescence

The new complexes prepared in this study PtL$^{10–15}$Cl are all brightly luminescent, emitting in the green–yellow region of the spectrum. Luminescence data for the new complexes, together with values for PtL^{1}Cl and PtL^{9}Cl, are summarised in Table 4. For the oxo-substituted series PtL$^{13–15}$Cl (Fig. S2 in the ESI†), the emission maxima are shifted a little towards the red, in line with the donating character of the phenolic oxygen atoms. Their emission properties are similar to PtL$^{1–8}$Cl, in that (i) the spectra are quite narrow, with some evidence of vibrational structure, (ii) they undergo self-quenching at elevated concentrations (k_Q = 2–5 × 10^9 M^{-1} s^{-1}) which is accompanied by the appearance of

Table 4 Luminescence data for the platinum complexes, in CH_2Cl_2 solution at 298 K

Complex and substituent	Emission λ_{max}/nm	Φ_{lum}[a] degassed	τ_0/μs[b] degassed	k_Q^{SQ}[b]/10^9 $M^{-1}s^{-1}$	k_Q^{O2}[c]/10^8 $M^{-1}s^{-1}$	Φ $^1O_2$[d,f]
PtL^1Cl[e] H–	491, 524, 562	0.60	7.2	5.3	9.1	0.65
PtL^9Cl[e] Me_2N-C_6H_4–	588	0.46	12	0.12	24	0.34
$PtL^{10}Cl$ Ph_2N-C_6H_4–	557	0.29	9.0	0.29	21	0.24
$PtL^{11}Cl$ (*p*-MeO-C_6H_4)$_2$N-C_6H_4–	572	0.30	11	0.53	37	0.26
$PtL^{12}Cl$ azacrown	580	0.28	9.5	< 0.10	23	0.30
$PtL^{13}Cl$ MeO-C_6H_4–	528, 555 sh	0.44	9.6	2.7	13	—
$PtL^{14}Cl$ $(MeO)_2$-C_6H_3–	533, 560 sh	0.49	11	4.5	16	0.55
$PtL^{15}Cl$ oxacrown	529, 560 sh	0.37	10	2.5	14	—

[a] Luminescence quantum yield determined using $[Ru(bpy)_3]Cl_2$ as the standard. [b] τ_0 is the lifetime at infinite dilution and k_Q^{SQ} the self-quenching rate constant, determined from the intercept and slope, respectively, of a plot of the measured decay rate constant against concentration. [c] Bimolecular rate constant for quenching by molecular oxygen, assuming that $[O_2] = 2.2 \times 10^{-3}$ M in CH_2Cl_2 at 1 atm air. [d] Quantum yield of singlet oxygen formation measured using perinaphthenone as the standard. [e] Data for PtL^1Cl and PtL^9Cl from references 12 and 13 respectively, except for Φ $^1O_2$ (this work). [f] Quantum yields of $^1O_2$ formation have also been measured during this work for the previously synthesised series of complexes: PtL^2Cl, 0.55; PtL^3Cl, 0.78; PtL^5Cl, 0.60; PtL^6Cl, 0.56; PtL^7Cl, 0.61; PtL^8Cl, 0.43.

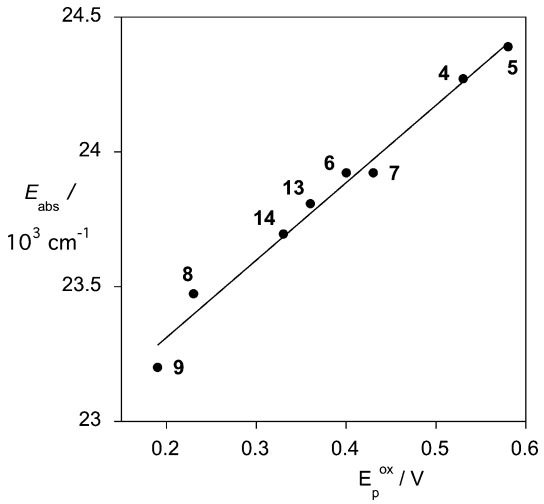

Fig. 4 Plot of the energy of the lowest-energy spin-allowed absorption maximum E_{abs} (in CH_2Cl_2) against the oxidation peak potential E_p^{ox} (in 90% CH_3CN–10% CH_2Cl_2) for the aryl-substituted complexes at 298 K, highlighting the remarkably linear correlation. The straight line represents the best fit through the data, gradient = 2900 cm^{-1}/V.

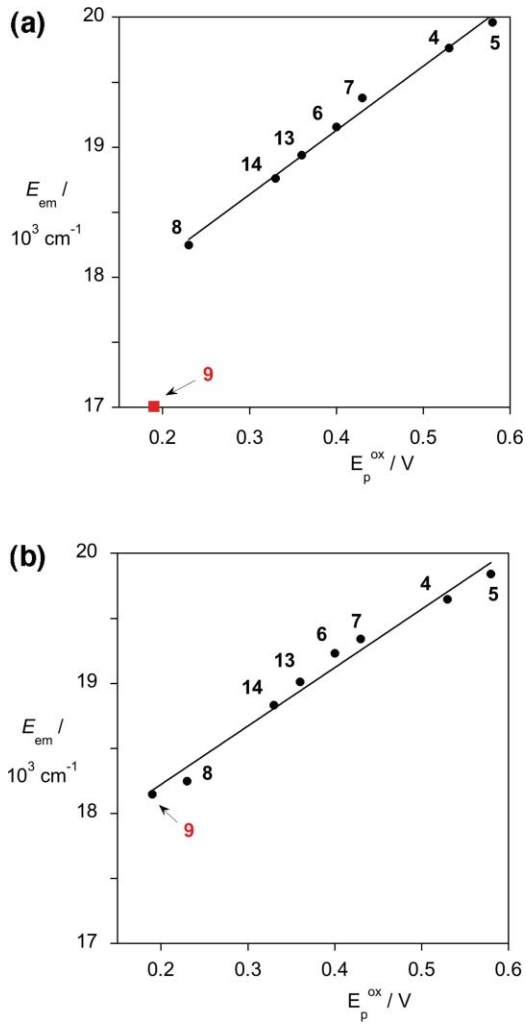

Fig. 5 Plot of the emission energy of the complexes in (a) dichloromethane, and (b) toluene, against the oxidation peak potential (in 90% CH_3CN–10% CH_2Cl_2 for both plots) at 298 K. The solid lines represent the best fit to the data, excluding (a), and including (b), the data point for PtL^9Cl; the respective gradients are 4900 and 4500 cm^{-1}/V.

a brightly emissive excimer band centred around 700 nm; and (iii) they are weakly negatively solvatochromic. These features in common with the previously investigated complexes suggest that the emission emanates from essentially the same type of excited state, and that the shift to the red can be interpreted in terms of the electron-donating nature of the substituents raising the energy of the HOMO, as for the singlet excitations in absorption. Indeed, when the emission energy E_{em} of the collective series of complexes in dichloromethane is plotted against E_p^{ox}, a remarkably linear correlation is observed (Fig. 5a), mirroring the trend found in absorption.

The anomalous behaviour of PtL^9Cl: solvent-induced switching of excited states. Despite the largely good correlation between E_{em} and E_p^{ox}, the emission energy of PtL^9Cl is anomalously low (Fig. 5a), lying well below the extrapolated line based on the other complexes. In contrast, we find that, for the corresponding plot of emission energies in toluene, PtL^9Cl appears at the 'expected' position based on its E_p^{ox} value, as it did in absorption (Fig. 5b). This suggests that there may be some additional stabilisation of the excited state of this complex in CH_2Cl_2, that does not apply

to the other complexes, or a switch to a different type of excited state.

Previously, we had noted that the emission of PtL^9Cl appeared to be anomalous in some other respects too:[13] (i) it displays strong positive solvatochromism, (varying by almost 4000 cm^{-1} between CCl_4 and MeCN), as opposed to the weak negative solvatochromism of the other complexes; (ii) the emission band is broad and structureless in CH_2Cl_2 and MeCN, but has the characteristic, partially structured profile in CCl_4 and toluene, similar to that of the other complexes; (iii) shows much less propensity to self-quenching or excimer formation than the other complexes, at elevated concentrations in CH_2Cl_2.

We have sought to probe in more detail whether the nature of the emissive excited state of PtL^9Cl does indeed change on going from CH_2Cl_2 to toluene. The limited solubility of the complex in toluene limits the range of concentrations available in this solvent. However, it proves to be informative to compare the emission properties in CH_2Cl_2 with those in 95% toluene–5% CH_2Cl_2. Comparison of the emission spectrum in dilute and concentrated solution in CH_2Cl_2 reveals only a little difference between the profiles (Fig. 6a, 40-fold difference in concentration): there is a slightly increased intensity in the red-end tail of the spectrum, which could be due to an excimer, but clearly only a small proportion relative to the monomeric species. Similarly, the lifetime of emission is reduced by only a relatively small factor of ~2 over this large concentration range. In contrast, in 95% toluene–5% CH_2Cl_2, the more concentrated solution displays a broad, low-energy band centred around 700 nm resembling that displayed by the other complexes and attributable to an excimer (Fig. 6b). The greater extent of intermolecular interaction in toluene is also manifest in the larger influence of concentration on the lifetime of the monomer band, falling from 11 to 1.4 μs over the 40-fold range displayed in Fig. 6b. Meanwhile, the decay kinetics registered at 700 nm reveal a clear-cut grow-in of the emission not observed for the same wavelength in CH_2Cl_2 (Fig. 6c), in line with bimolecular excimer formation in the former solvent.

Thus, the observations collectively point to a change in the nature of the emissive excited state of PtL^9Cl in the more polar solvents (CH_2Cl_2 and CH_3CN), to one in which the intermolecular interactions that lead to excimers are inhibited. A change to a state with a more complete transfer of charge from the amino pendant to the core of the complex seems likely, perhaps reminiscent of the Twisted Intramolecular Charge Transfer (TICT) states of structurally related organic molecules like *p*-dimethylaminobenzonitrile, which are sufficiently stabilised in more polar solvents to become the lowest-energy excited states.[21] Although the exact nature of such states remains the subject of much fascinating experimental and theoretical study,[22] the general consensus is in favour of a twisted model, in which the initially formed locally excited state undergoes a radiationless reorganisation in polar solvents to a state in which the dimethylamino group is perpendicular to the ring, and hence electronically decoupled, accompanied by transfer of charge to the acceptor terminus. Thus, whilst the emission of such molecules is usually strongly solvatochromic, the absorption may be much less so, as is indeed the case for PtL^9Cl.

Meanwhile, McMillin and co-workers have noted that the introduction of ILCT character in 4-amino-substituted platinum terpyridyl complexes substantially reduces their tendency to

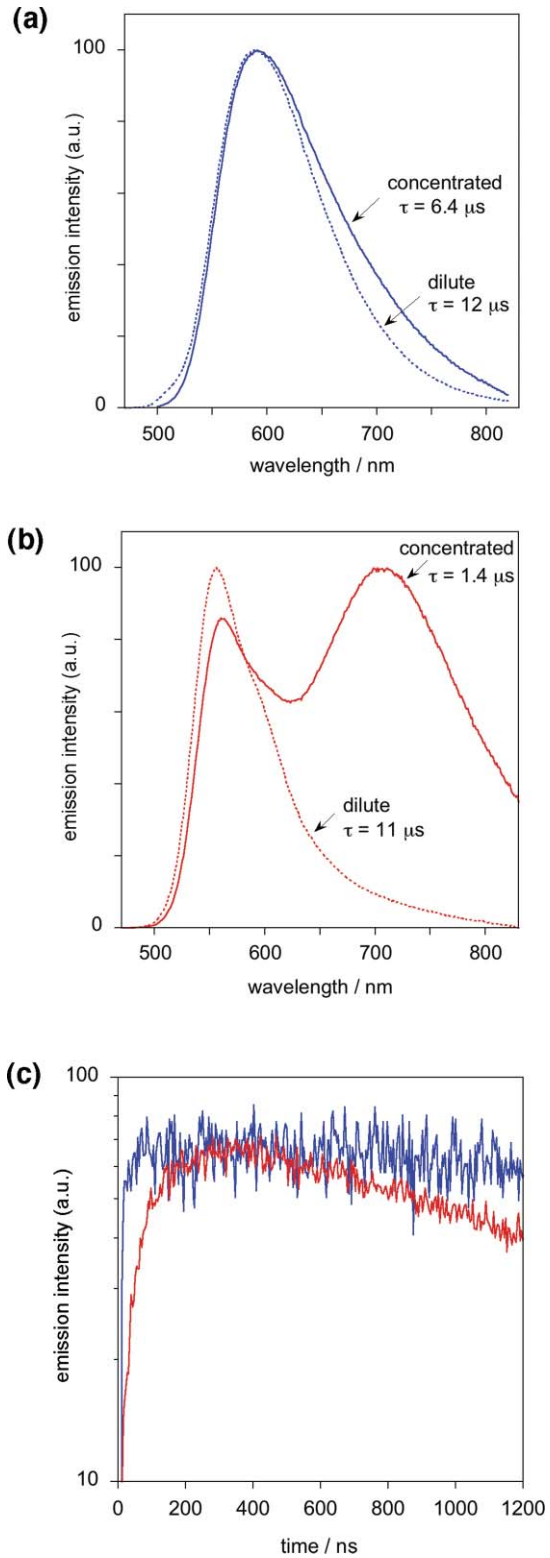

Fig. 6 (a) Emission spectra of PtL^9Cl in CH_2Cl_2 at concentrations of 1×10^{-5} M (dotted line) and 4×10^{-4} M (solid line). (b) The corresponding spectra at the same concentrations in toluene, revealing the formation of a strongly emissive excimer. (c) Decay kinetics of emission of PtL^9Cl registered at 700 nm in the concentrated solutions (4×10^{-4} M) in dichloromethane (blue) and toluene (red), highlighting the grow-in of the excimer in toluene only.

undergo quenching reactions with donating solvents such as acetonitrile, probably because of the increased electron density at the metal.[8a,23] A similar effect in the present instance might reasonably account for the lower propensity to excimer fomation in CH_2Cl_2.

If the above interpretation is correct, then the dipole moment of the emissive triplet state of the compound should be larger in CH_2Cl_2 than in toluene, owing to a greater degree of charge separation. The change in dipole moment of a molecule upon formation of an excited state can frequently be probed by Stark electroabsorption spectroscopy—in which the influence of a strong electric field on the absorption transitions is probed—but the technique is limited to excited states that are formed directly from the ground state upon excitation, *viz.* normally the singlet states.[24] In the present case, the emissive triplet states are formed subsequent to light absorption, by intersystem crossing from the singlet. The related technique of transient DC photoconductivity (TDCP) can allow such states to be probed.[25,26] Briefly, the change in capacitance of a cell containing a solution of the compound, across which is applied a strong electric field, is monitored during, and immediately following, pulsed laser excitation. Any difference between the dipole moment in the excited compared to the ground state will result in the molecules realigning within the electric field, equivalent to transient flow of charge. The TDCP signal scales with $\mu_{ex}^2-\mu_{gd}^2$. TDCP data obtained for PtL^9Cl in toluene could be fitted satisfactorily on the basis of $(\mu_{ex}^2-\mu_{gd}^2) = 150$ (±20) Debye^2 and $\tau_{ex} = 12$ μs, the latter value being fully consistent with the observed lifetime (a representative TDCP photoresponse and fit is shown in the ESI†, Fig. S4). Attempts to measure the response in CH_2Cl_2 were unsuccessful, owing to breakdown of the solvent under the applied electric field. However, data could be obtained in 1,2-dichloroethane, a similar solvent both in terms of chemical composition and polarity, giving a value of $(\mu_{ex}^2-\mu_{gd}^2) = 250$ (±20) Debye.^{2} The significantly larger value in the latter solvent is consistent with the notion of a greater extent of charge transfer under more polar conditions.

Triplet state inversion according to solvent has recently been described by Castellano *et al.* in a very different class of platinum(II) complexes.[27] They noted that in Pt(dbbpy)(–C≡C–ϕ–C≡C–ϕ–C≡C–Ph)$_2$, emission from a ^{3}CT state was observed only in the least polar solvents (e.g. *n*-hexane) whereas emission from a ^{3}IL state localised on the acetylides dominates under more polar conditions. In their case, the ^{3}CT increases in energy with increasing solvent polarity, and the effect is more readily probed on the basis of the variation in the decay kinetics as a function of solvent polarity, because of the large difference in magnitudes of the lifetimes of the two types of excited state.

Although the DFT calculations on PtL^9Cl do not reveal evidence for such a twisted state becoming lowest in energy in dichloromethane (the amine group being essentially coplanar with the phenyl ring in the energy-minimised geometry), it should be noted that the difference in energy involved is small, ~1000 cm^{-1} (0.12 eV) on the basis of the data trend in Fig. 5a, and clearly very sensitive to the solvent. Moreover, states with an extensive degree of charge separation—of which the proposed TICT-like state would be one—are generally poorly modelled by B3LYP, especially when the occupied and virtual orbitals involved in the excitation do not overlap.[28]

Diarylamine complexes. Intrigued whether this behaviour would also be seen for complexes with slightly less electron-rich, diarylamine pendants (as opposed to the dialkylamino unit of PtL^9Cl), we investigated the complexes $PtL^{10}Cl$ and $PtL^{11}Cl$. In dichloromethane solution, the emission energies lie in the order $PtL^{10}Cl > PtL^{11}Cl > PtL^9Cl$ (Fig. 7), in line with the expected order of increasing electron-donating ability of the amine, but the emission spectral profiles, lifetimes and self-quenching constants of the arylamine complexes are all similar to those of PtL^9Cl, suggesting that they too have more ILCT character in this solvent. Careful inspection of the spectra at high concentration compared to dilute solution does, however, reveal a little more marked concentration dependence than PtL^9Cl, with somewhat enhanced low-energy emission, whilst the self-quenching rate constants are actually a little larger for the arylamine complexes, despite the larger expected steric bulk, suggesting that the switch to TICT behaviour is somewhat less clear-cut for these complexes.

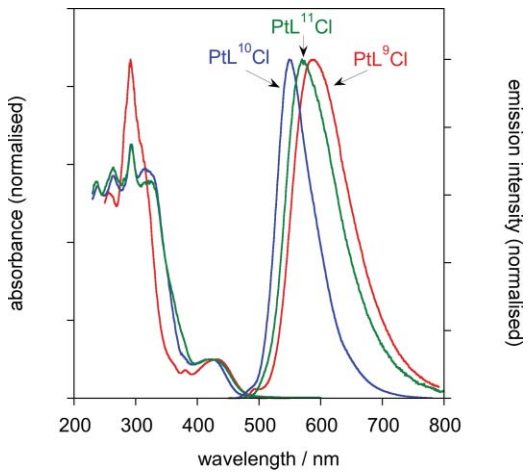

Fig. 7 Absorption and emission spectra of the diarylamino complexes $PtL^{10}Cl$ (blue) and $PtL^{11}Cl$ (green) in CH_2Cl_2 at 298 K, together with that of PtL^9Cl (red) for comparison.

5. Chemically-induced switching of excited states: an azacrown-substituted complex $PtL^{12}Cl$

In our previous study, we noted that the addition of acid to a dichloromethane solution of PtL^9Cl leads to a substantial shift in both the emission band and the lowest-energy absorption band to higher energy: λ_{max}^{abs} shifts from 431 to 410 nm; λ_{max}^{em} from 588 to 482 nm.[13] The effect is reversed upon addition of an organic base such as $Me_4N^+OH^-$. These changes are clearly due to the fact that protonation of the pendant amine nitrogen atom will attenuate or even essentially eliminate its participation in the molecular orbital previously identified as HOMO in Fig. 1(b). The HOMO will now return to being centred primarily on the N^C^N unit, as in PtL^1Cl, restoring the localised π–π* state as the emissive state; indeed, the emission characteristics of $[PtL^9HCl]^+$ are similar to those of PtL^1Cl.[13]

We sought to investigate whether this modulation of the excited states could be extended to other systems, triggered by species other than the proton. Reversible switching between excited states with significantly different emission properties, induced by target analytes, can be exploited in ratiometric sensing applications, for

example, as in many of the calcium sensors used in physiological studies.[29] As a proof of principle, we chose to prepare the azacrown-substituted complex PtL^{12}Cl. The azacrown unit is well-known to bind several divalent metal ions, M^{n+}, a process that involves the use of the lone pair on the azacrown nitrogen atom.[30] The positioning of the latter at the position corresponding to the N atom in PtL^{9}Cl should lead to metal-ion triggered modulation of emission.

In the absence of added metal ions, the excited state properties of PtL^{12}Cl are indeed very similar to those of PtL^{9}Cl (Tables 3 and 4). TD-DFT calculations confirm that the azacrown has a directly analogous effect to the –NMe_2 unit, as shown by the assignments and calculated energies of the lowest-lying singlet and triplet transitions listed in Table 2, which are very similar for the two complexes.

The absorption and emission spectra of PtL^{12}Cl were monitored as a function of added group I (Li^+, Na^+ and K^+) and group II (Mg^{2+}, Ca^{2+} and Ba^{2+}) metal ions and Zn^{2+} in air-equilibrated MeCN at room temperature. This solvent was selected owing to the greater solublity of metal triflate salts therein compared to dichloromethane. Little effect was observed for the group I metal ions, but the divalent metal ions led to a marked change in the emission spectrum, which shifted substantially to higher energy and increased in intensity. The strongest response was observed for calcium; the emission spectra prior to and after addition of an excess of Ca^{2+} are shown in Fig. 8. The observed change is evidently directly analogous to the effect of protonation on PtL^{9}Cl, and can be interpreted in terms of the inversion of the relative energies of the N^C^N-localised and TICT excited states. Thus, upon binding of Ca^{2+} to the pendent amine, the latter is increased in energy such that the former becomes the emissive state (Scheme 2).

In contrast to the profound effect on the triplet state luminescence, the change in the absorption spectrum in the presence of an excess of Ca^{2+} is less pronounced, with the lowest-energy band shifting only from 426 to 414 nm (Fig. 8). This is consistent with the observation described earlier that the absorption of the amine complex PtL^{9}Cl lies in line with the absorbance maxima of the other complexes on the basis of E_p^{ox} (Fig. 3): it is only for the emissive excited state where the additional stabilisation is observed for this complex (Fig. 5a).

Somewhat related examples of how the excited states of azacrown-substituted platinum complexes can be modulated by ion binding have been reported by Yam and by Wu.[11] They have studied complexes of the type [Pt(tpy)(–C≡C–Ar)]$^+$ or

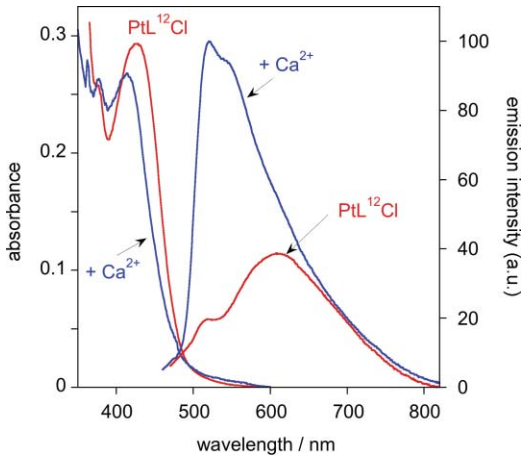

Fig. 8 Absorption and emission spectra of PtL^{12}Cl (3.6×10^{-5} M) in air-equilibrated MeCN (containing Bu_4NClO_4, 0.1 M, as inert electrolyte) (red lines), and corresponding spectra in the presence of calcium triflate (1×10^{-3} M) (blue lines); $\lambda_{ex} = 374$ nm (isosbestic point), $T = 298$ K.

[Pt(phbpy)(–C≡C–Ar)] where Ar is a unit such as benzo-18-crown-5 or 15-monoazacrown-5. In these cases, the emission of the unbound form is very low, either because it involves an ILCT state that is of low-energy and subject to efficient non-radiative decay, or because of quenching of the excited state by photoinduced electron transfer from the amine lone pair. The compounds thus function as "turn-on" sensors. The present system differs and, indeed, is unusual amongst azacrown-appended lumophores in general, in that both forms are highly emissive, and the metal binding leads to a clear-cut shift in the spectrum, and not just to an intensity change.

6. Benzo-18-crown-6-substituted complex, PtL^{15}Cl

The oxacrown-substituted complex PtL^{15}Cl displays similar luminescence properties to the dimethoxyphenyl-substituted complex PtL^{14}Cl, as expected. The modulation of the absorption and emission spectra of this complex in response to added divalent metal cations M^{2+} was investigated. Experiments were carried out in MeCN solution, using the same metal triflate salts as those screened in the study of PtL^{12}Cl. Again, little effect was observed for the group I metal ions. The divalent metal ions Mg^{2+}, Ca^{2+} and Zn^{2+} led to a blue-shift in the lowest-energy spin-allowed

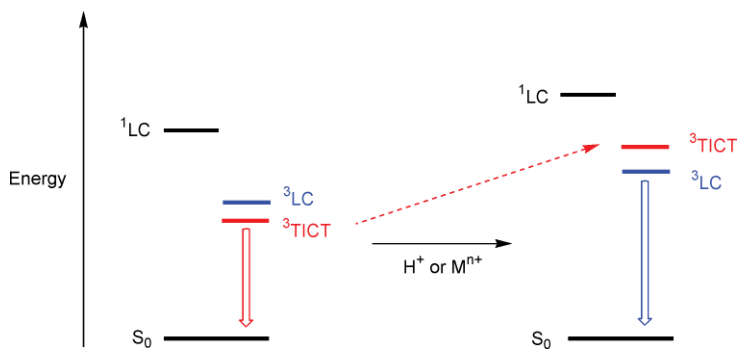

Scheme 2 Schematic illustration of the proposed effect of binding of H^+ or metal ions such as Ca^{2+} upon the relative energies of the ligand-centred and intramolecular charge-transfer excited states in complexes PtL^{9}Cl and PtL^{12}Cl.

absorption band, which was most significant for Zn^{2+} (Fig. 9). This effect can again be interpreted in terms of the influence of metal binding on the phenolic oxygen atoms, which will render them less electron-donating and hence lower the HOMO energy, shifting the excitations towards the higher energies observed for PtL^1Cl. On the other hand, the emission band—though showing some decrease in intensity upon addition of metal ions—displays no shift: the profile is unchanged (Fig. 9). This might suggest that the affinity of the excited state for the metal ions is lower than that of the ground state, a plausible possibility given the redistribution of electron density away from the crown and towards the platinum centre upon excitation.

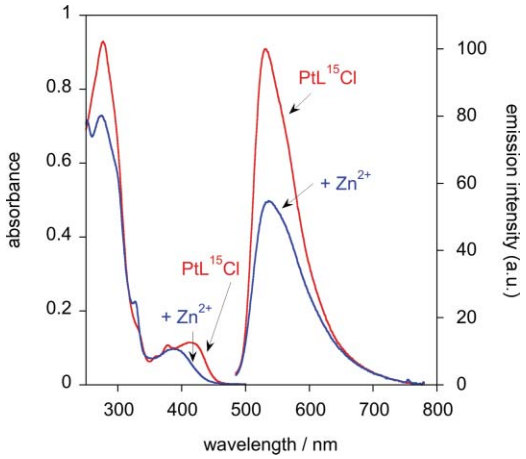

Fig. 9 Absorption and emission spectra of the benzo-18-crown-6 appended complex, $PtL^{15}Cl$ (1.7×10^{-5} M) in MeCN solution (containing 0.1 M Bu_4NClO_4 as an inert electrolyte) (red lines), and the corresponding spectra in the presence of zinc triflate (5×10^{-4} M) (blue lines); $\lambda_{ex} = 365$ nm (isosbestic point), $T = 298$ K.

7. Oxygen sensitivity and $^1O_2$ formation

The luminescence of all of the complexes in solution is partially quenched by dissolved molecular oxygen, with bimolecular rate contants of the order of 10^9 $M^{-1}s^{-1}$ in CH_2Cl_2 at 298 K (Table 4). The values are largest for the most electron-rich, amino-substituted complexes. The triplet states of many transition metal complexes can act as sensitisers of singlet oxygen, O_2 $^1\Delta_g$, by energy transfer to the $^3\sum_g^-$ ground state of molecular oxygen. For the present set of complexes, the quenching of the visible luminescence by oxygen was accompanied by the appearance of emission in the near-IR, attributable to the formation and subsequent radiative decay of the $^1\Delta_g$ state, which emits at ~1270 nm. The quantum yields of singlet oxygen formation by the complexes in CH_2Cl_2 under irradiation at 355 nm were determined using perinaphthenone as a standard.[31] With the exception of PtL^9Cl and $PtL^{12}Cl$, no significant quenching of the generated singlet oxygen by the complexes was observed: the rate of decay of the $^1\Delta_g$ emission in the near-IR was 1.2×10^4 s^{-1}, essentially identical to that measured following production *via* the standard. In the case of the Me_2N, and azacrown–substituted complexes, however, the rate of decay of the $^1O_2$ was increased by a factor of around 2, corresponding to a bimolecular quenching rate constant of ~5×10^8 $M^{-1}s^{-1}$. Although some transition metal complexes are known to quench $^1O_2$ once generated,[32] the fact that this effect is observed only for these two systems amongst the family of complexes suggests some chemical reactivity associated with the basic dialkylamino units, possibly N-oxidation. In line with this result, we also note an empirical observation that these two complexes display evidence of long-term instability: over a period of days in aerated solution, a new high-energy band appears in the emission spectrum centred around 510 nm, at the expense of the original emission band, which would be consistent with amine oxidation or cleavage.

Thus, whilst it might be tempting to suggest that complexes such as $PtL^{12}Cl$ could be viable luminescent sensors for metal ions, amenable to time-resolved detection procedures owing to their long lifetimes, the development of such systems to practicable applications would face tough challenges. In particular, the oxygen sensitivity, singlet oxygen generation, and questionable long-term stability would all compromise the potential performance.

Summary and conclusions

The new compound 1,3-di(2-pyridyl)-5-boronic acid neopentylglycolate, dpyb-B, has been shown to be a versatile intermediate for the preparation of 5-aryl-appended N^C^N-binding ligands. The new ligands prepared in this study—which incorporate a variety of electron rich aromatics with amino and alkoxy substituents—all lead to highly luminescent platinum(II) complexes. They have quantum yields in solution in the range 0.3–0.5 and lifetimes of the order of 10 μs at room temperature. Density functional theory calculations which include the effect of the solvent demonstrate remarkable success in simulating observed absorption spectra, and confirm that the trend to lower excited-state energies upon aryl substitution is associated with the participation of the pendant group in the HOMO. In dichloromethane solution, the lower-than-anticipated emission energy of the amino complexes is probably due to the stabilisation of a TICT-like state under the more polar conditions. By incorporating the amine atom into an azacrown, the effect can be reversed through the binding of divalent metal ions such as Ca^{2+}, leading to the profound changes in emission profile observed. In contrast, there is no change in emission profile upon binding of metal ions to the oxocrown analogues, despite a shift of the absorption to higher energies. All the complexes are shown to be very efficient sensitisers of the $^1\Delta_g$ state of oxygen in solution. Overall, the results demonstrate the rich potential of the family of N^C^N-coordinated platinum(II) complexes, and the ability to switch between different excited states—each highly luminescent—with distinct properties through simple stuctural modification.

Experimental

Proton and ^{13}C NMR spectra, including NOESY and COSY, were recorded on Varian 300, 400 or 500 MHz instruments. Chemical shifts (δ) are in ppm, referenced to residual protio-solvent resonances, and coupling constants are in Hertz. Electron ionisation (EI) mass spectra were recorded with a Micromass AutoSpec spectrometer. Electrospray ionisation (ES) mass spectra were acquired on a time-of-flight Micromass LCT spectrometer with methanol or acetonitrile as the carrier solvent. All solvents used in preparative work were at least Analar grade, and water

was purified using the Purite® system. Solvents used for optical spectroscopy were HPLC grade.

1,3-Di(2-pyridyl)benzene (HL[1]) and 1,3-di(2-pyridyl)-5-bromobenzene (dpyb-Br) were prepared by palladium-catalysed reaction of 2-(tributylstannyl)-pyridine with 1,3-dibromobenzene and 1,3,5-tribromobenzene respectively, as described previously.[33,13] 4-Bromo-*N*,*N*-diphenylaniline was prepared by a modified Ullmann coupling from diphenylamine and 4-bromoiodobenzene;[34] the dianisyl analogue was prepared in the same way. 1,3-Di(2-pyridyl)-5-(*p*-dimethylaminophenyl)benzene, HL[9], was prepared by Suzuki cross-coupling of dpyb-Br with *p*-(dimethylamino)phenylboronic acid; data were identical to those from the different method of preparation used in our previous work, in which the Stille and Suzuki reactions were carried out in the opposite sequence.[13] The synthesis and characterisation of 4-bromophenyl-*N*-monoaza-15-crown-5 are described in the ESI†.

1,3-Di(2-pyridyl)benzene-5-boronic acid neopentylglycol ester (dpyb-B)

A mixture of dpyb-Br (110 mg 0.34 mmol), potassium acetate (118 mg, 1.20 mmol), bis(neopentyl glycolato)-diboron (87 mg, 0.39 mmol) and 1,1′-[bis(diphenylphosphino)]ferrocene palladium(II) dichloride (20 mg, 0.027 mmol) in anhydrous DMSO (5 mL) was degassed by three freeze–pump–thaw cycles and back-filled with nitrogen. The mixture was heated at 80 °C for 6 h under nitrogen. After cooling to ambient temperature, toluene (15 mL) was added, and the solution washed with water (5 × 20 mL). The organic layer was dried over anhydrous potassium carbonate, filtered and the solvent removed under reduced pressure to give a pale brown solid, which was recrystallised from dichloromethane–methanol solution to give the product (114 mg, 90%). ^{1}H NMR (500 MHz, $CDCl_3$): δ 8.74 (1H, t, ^4J 1.5, H$^{2'}$), 8.72 (2H, dd, ^3J 5.0, ^4J 1.5, H^6), 8.48 (2H, d, ^4J 1.5, H$^{4'}$), 7.89 (2H, dt, ^3J 8.0, ^4J 1.5, H^3), 7.76 (2H, td, ^3J 8.0, ^4J 2.0, H^4), 7.23 (2H, ddd, ^3J 7.5, ^3J 5.0, ^4J 1.5, H^5), 3.82 (4H, s, –CH_2–), 1.05 (6H, s, CH_3). ^{13}C NMR (126 MHz, $CDCl_3$): δ 157.7, 149.8 (C^6), 139.3, 136.8 (C^4), 133.1 (C$^{2'}$), 128.1 (C$^{4'}$), 122.2 (C^5), 121.0 (C^3), 72.49 (CH_2), 32.1 (C-alkyl quat), 22.1 (CH_3). HRMS (ES$^+$): *m*/*z* 345.17702 [M + H]$^+$; [$C_{21}H_{22}N_2O_2{}^{11}B$] requires 345.17689.

5-(4-*N*,*N*-Diphenylaminophenyl)-1,3-di(2-pyridyl)benzene HL[10]

A mixture of dpyb-B (178 mg, 0.52 mmol), 4-bromo-*N*,*N*-diphenylaniline (169 mg, 0.52 mmol), and sodium carbonate (66 mg, 0.62 mmol, in 0.2 mL water), in dimethoxyethane (10 mL) was degassed and back-filled with nitrogen gas. Tetrakis(triphenylphosphine)palladium(0) (48 mg, 0.042 mmol) was added under a stream of nitrogen, and the mixure was heated at 80 °C for 60 h. The solvent was then removed under reduced pressure, and the residue taken into dichloromethane (40 mL) and washed with water (4 × 30 mL). After separation of the organic layer and drying over anhydrous potassium carbonate, the solvent was evaporated and the residue purified by chromatography on silica gel, gradient elution from hexane to 80 : 20 hexane : diethyl ether (R_f = 0.4 in 75 : 25 hexane : diethyl ether), followed by recrystallisation from hexane : diethyl ether yielding a colourless solid (76 mg, 31%). ^{1}H NMR (400 MHz, $CDCl_3$): δ 8.75 (2H, dd, ^3J 5.0, ^4J 1.5, H^6), 8.57 (1H, t, ^4J 1.5, H$^{2'}$), 8.29 (2H, ^4J 1.5, H$^{4'}$), 7.93 (2H, d, ^3J 8.0, H^3), 7.82 (2H, td, ^3J 7.5, ^4J 1.5, H^4), 7.66 (2H, d, ^3J 8.5, H^b), 7.29 (6H, m, H$^{a'}$, H^5), 7.18 (4H, d, ^3J 8.5, H$^{b'}$), 7.15 (2H, m, H^a), 7.04 (2H, t, ^3J 7.5, H$^{c'}$). MS (ES$^+$): *m*/*z* 476 [M + H]$^+$. Anal. calcd. for $C_{36}H_{29}N_3O_2$: C, 80.7; H, 5.5; N, 7.8%. Found C, 80.3; H, 5.7; N, 7.5%.

5-[4-*N*,*N*-Di(4-methoxyphenyl)aminophenyl]-1,3-di(2-pyridyl)benzene HL[11]

Compound HL[11] was prepared used the same procedure as for HL[10], using dpyb-B (290 mg, 0.84 mmol) and 4-bromo-*N*,*N*-di(anisyl)aniline (301 mg, 0.78 mmol). Work-up and purification by chromatography on silica using the same eluant as for HL[10] gave the product as a colourless solid (111 mg, 25%). ^{1}H NMR (400 MHz, $CDCl_3$): δ 8.76 (2H, d, ^3J 4.5, H^6), 8.59 (1H, s, H$^{2'}$), 8.31 (2H, s, H$^{4'}$), 7.98 (2H, d, ^3J 8.0, H^3), 7.88 (2H, t, ^3J 7.5, H^4), 7.63 (2H, d, ^3J 8.5, H^b), 7.35 (2H, m, H^5), 7.12 (4H, d, ^3J 8.5, H$^{b'}$), 7.05 (2H, d, H^a), 6.89 (4H, d, ^3J 8.5, H$^{a'}$), 3.81 (CH_3). MS (ES$^+$): *m*/*z* 536 [M + H]$^+$. Anal. Calcd. for $C_{34}H_{25}N_3$: C, 85.9; H, 5.3; N, 8.8%. Found C, 86.0; H, 5.4; N, 8.2%.

5-[4-(*N*-Monoaza-15-crown-5)phenyl]-1,3-di(2-pyridyl)benzene HL[12]

This compound was prepared in the same way as HL[10] using dpyb-B (154 mg, 0.45 mmol), 4-bromophenyl-*N*-monoaza-15-crown-5 (93 mg, 0.25 mmol), sodium carbonate (37 mg, 0.35 mmol) and $Pd(PPh_3)_4$ (34 mg, 0.029 mmol) in a mixture of toluene : ethanol : water (3 : 3 : 1 mL respectively). The mixture was heated at 80 °C for 3 d before work up as for HL[10]. The crude product was purified by chromatography on aluminium oxide, gradient elution from hexane to 70 : 30 hexane : ethyl acetate (R_f = 0.8 in ethyl acetate) yielding a clear oil (122 mg, 88%). ^{1}H NMR (300 MHz, $CDCl_3$): δ 8.73 (2H, d, ^3J 4.5, H^6), 8.48 (1H, t, ^4J 1.5, H$^{2'}$), 8.23 (2H, d, ^4J 1.5, H$^{4'}$), 7.88 (2H, d, ^3J 8.0, H^3), 7.78 (2H, td, ^3J 8.0, ^4J 1.7, H^4), 7.65 (2H, d, ^3J 8.5, H^b), 7.26 (2H, dd, ^3J 5.0, ^4J 1.0, H^5), 6.76 (2H, d, ^3J 8.5, H^a), 3.80 (4H, t, ^3J 6.0) and 3.66 (16H, m), alicyclic protons. MS (ES$^+$): *m*/*z* 547 [M + Na]$^+$, 526 [M + H]$^+$.

5-(4-Methoxyphenyl)-1,3-di(2-pyridyl)benzene HL[13]

This compound was prepared from dpyb-Br (106 mg, 0.34 mmol), 4-methoxyphenylboronic acid (58 mg, 0.38 mmol), sodium carbonate (149 mg, 1.41 mmol) and $Pd(PPh_3)_4$ (40 mg, 0.035 mmol), suspended in a mixture of toluene : ethanol : water (4 : 4 : 1 mL respectively). The mixture was heated at 80 °C for 60 h. Purification was performed by chromatography on silica gel, elution 50 : 50 hexane : diethyl ether (R_f = 0.7 in diethyl ether) followed by recrystalisation from hexane (121 mg, 94%). ^{1}H NMR (500 MHz, $CDCl_3$): δ 8.74 (2H, dd, ^3J 5.0, ^4J 1.5, H^6), 8.54 (1H, t, ^4J 1.5, H$^{2'}$), 8.26 (2H, d, ^4J 1.5, H$^{4'}$), 7.89 (2H, d, ^3J 7.5, H^3), 7.79 (2H, td, ^3J 7.5, ^4J 1.5, H^4), 7.71 (2H, d, ^3J 8.5, H^b), 7.27 (2H, dd, ^3J 6.0, ^3J 4.5, H^5), 7.01 (2H, d, ^3J 8.5, H^a), 3.87 (3H, s, CH_3). ^{13}C NMR (126 MHz, $CDCl_3$): δ 159.5, 157.4, 149.8 (C^6), 142.0, 140.5, 136.9 (C^4), 133.5, 128.6 (C^a), 126.1 (C$^{4'}$), 124.1 (C$^{2'}$), 122.5 (C^5), 121.0 (C^3), 114.3 (C^b), 55.5 (CH_3). HRMS (ES$^+$): *m*/*z* 339.14903 [M + H]$^+$, [$C_{23}H_{19}N_2O$] requires 339.14919.

5-(3,4-Dimethoxyphenyl)-1,3-di(2-pyridyl)benzene HL[14]

Ligand HL[14] was prepared as described for HL[13], using 3,4-dimethoxyphenylboronic acid (103 mg, 0.57 mmol) in place of methoxyphenylboronic acid. Purification by chromatography on silica gel, elution gradient from hexane to diethyl ether ($R_f = 0.5$ in diethyl ether), yielded a colourless solid, which was recrystallised from diethyl ether (64 mg, 31%). ^{1}H NMR (500 MHz, $CDCl_3$): δ 8.75 (2H, d, ^3J 4.5, H^6), 8.55 (1H, t, ^4J 1.5, H$^{2'}$), 8.27 (2H, d, ^4J 1.5, H$^{4'}$), 7.92 (2H, d, ^3J 8.0, H^3), 7.82 (2H, td, ^3J 7.5, ^4J 1.5, H^4), 7.31 (4H, m, H^5, H^d, H^b), 6.98 (1H, d, ^3J 8.0, H^a), 4.00 (3H, s, *m*-CH_3), 3.94 (3H, s, *p*-CH_3). ^{13}C NMR (126 MHz, $CDCl_3$): δ 157.3, 149.7 (C^6), 149.2, 148.9, 142.3, 140.4, 137.0, 134.0, 126.2 (C$^{4'}$), 124.2 (C$^{2'}$), 122.5 (C^5), 121.0 (C^3), 119.9, 111.5 (C^a), 110.7, 56.2 (*m*-CH_3), 56.1 (*p*-CH_3). MS (ES$^+$): *m*/*z* 369.3 [M + H]$^+$.

5-(3,4-Benzo-18-crown-6)-1,3-di(2-pyridyl)benzene HL[15]

HL[15] was prepared using the procedure used for HL[10–12], starting from dpyb-B (284 mg, 0.83 mmol), 4′-bromobenzo-18-crown-6 (337 mg, 0.86 mmol), sodium carbonate (119 mg, 1.12 mmol), and $Pd(PPh_3)_4$ (38 mg, 0.033 mmol) in a mixture of toluene : ethanol : water (6 : 6 : 1 mL). The mixture was heated at 80 °C for 80 h. Purification of the crude material by chromatography on aluminium oxide, gradient elution from hexane to ethyl acetate ($R_f = 0.3$ in ethyl acetate), yielded the product as a clear, colourless oil (192 mg, 43%). ^{1}H NMR (500 MHz, $CDCl_3$): δ 8.74 (2H, d, ^3J 4.5, H^6), 8.53 (1H, t, ^4J 1.5, H$^{2'}$), 8.23 (2H, d, ^4J 1.5, H$^{4'}$), 7.89 (2H, d, ^3J 7.5, H^3), 7.79 (2H, td, ^3J 7.5, ^4J 1.5, H^4), 7.28 (4H, m, H^b, H^d, H^5), 6.98 (1H, d, ^3J 8.0, H^a), 4.28 (2H, t, ^3J 4.5, H$^{\alpha'}$), 4.22 (2H, t, ^3J 4.5, H$^\alpha$), 3.96 (4H, t, ^3J 4.5, H$^\beta$, H$^{\beta'}$), 3.80 (4H, m, H$^\gamma$, H$^{\gamma'}$), 3.74 (4H, m, H$^\delta$, H$^{\delta'}$), 3.70 (4H, s, H$^\varepsilon$, H$^{\varepsilon'}$). ^{13}C NMR (126 MHz, $CDCl_3$): δ 157.4, 149.8, 149.3, 149.0, 142.2, 140.5, 137.0, 134.6, 126.3 (C$^{4'}$), 124.2 (C$^{2'}$), 122.5 (C^5), 121.1 (C^3), 120.6, 114.5 (C^b), 113.9 (C^d), 71.0, 71.0, 70.9, 69.9, 69.8, 69.6, 69.4. HRMS (ES$^+$): *m*/*z* 543.24895 [M + H]$^+$, [$C_{32}H_{35}N_2O_6$] requires 543.24896; *m*/*z* 565.23048 [M + Na]$^+$, [$C_{32}H_{34}O_6N_2{}^{23}$Na] requires 565.23090.

Platinum complexes

The platinum(II) complexes of the ligands were prepared by reaction with potassium tetrachloroplatinate(II) using one of two methods. For Pt[10–11]Cl and Pt[13–14]Cl, a mixture of the ligand (50–100 mg) and K_2PtCl_4 (1 equiv.) in acetic acid (typically 3 mL) was degassed by three freeze–pump–thaw cycles and back-filled with nitrogen gas. The mixture was refluxed for 72 h. The resulting yellow or orange precipitate was separated by centrifugation and washed successively with water, ethanol and diethyl ether (3 × 5 mL of each). The solid was then extracted into dichloromethane, filtered to remove small amounts of insoluble residue, and the solvent then evaporated to give the product. The complexes PtL^{9}Cl and Pt^{12}Cl, which feature basic nitrogen atoms in the pendants, as well as Pt^{15}Cl, were prepared by mixing a solution of the ligand in acetonitrile (typically 50 mg in 5 mL) with a solution of K_2PtCl_4 in water (1 equiv. in 2.5 mL), both of which had been previously purged with nitrogen gas, and refluxing the mixture under nitrogen for 72 h. Work-up was similar to that used for the preparations in acetic acid.

PtL^{10}Cl From HL[10] (76 mg, 0.16 mmol) giving a yellow solid (97 mg, 88%). ^{1}H NMR (400 MHz, $CDCl_3$): δ 9.35 (2H, d, ^3J 5.5, $^3J(^{195}$Pt) 39, H^6), 7.96 (2H, td, ^3J 7.5, ^4J 1.5, H^4), 7.74 (2H, dd, ^3J 8.0, ^4J 1.5, H^3), 7.61 (2H, s, H$^{3'}$), 7.50 (2H, d, ^3J 8.5, H^b), 7.29 (6H, m, H$^{a'}$, H^5), 7.16 (6H, m, H^a, H$^{b'}$), 7.05 (2H, tt, ^3J 7.0, ^4J 1.0, H$^{c'}$). ^{13}C NMR (101 MHz, $CDCl_3$): δ 167.3, 152.5, 147.7, 147.3, 141.4, 139.3 (C^4), 136.6, 135.8, 129.5, 127.7 (C^b), 124.5, 124.2, 123.5, 123.2 (C$^{c'}$), 123.1 (C$^{3'}$), 119.4 (C^3). Anal. Calcd. for $C_{34}H_{24}N_3PtCl$: C, 57.9; H, 3.4; N, 6.0%. Found C, 57.1; H, 3.4; N, 5.9%.

PtL^{11}Cl From HL[11] (81 mg, 0.15 mmol) giving a deep yellow solid (25 mg, 22%). ^{1}H NMR (400 MHz, $CDCl_3$): δ 9.38 (2H, d, ^3J 6.0, $J(^{195}$Pt) 40, H^6), 7.96 (2H, td, ^3J 7.5, ^4J 1.5, H^4), 7.75 (2H, d, ^3J 8.0, H^3), 7.60 (2H, s, H$^{3'}$), 7.44 (2H, d, ^3J 8.5, H^b), 7.29 (2H, m, H^5), 7.12 (4H, d, ^3J 7.0, H$^{b'}$), 7.03 (2H, d, H^a), 6.87 (4H, d, ^3J 7.0, H$^{a'}$). Anal. Calcd. for $C_{34}H_{24}N_3PtCl$: C, 57.9; H, 3.4; N, 6.0%. Found C, 57.1; H, 3.4; N, 5.9%.

PtL^{12}Cl From HL[12] (112 mg, 0.21 mmol) giving an orange solid (100 mg, 68%). ^{1}H NMR (500 MHz, $CDCl_3$): δ 9.28 (2H, d, ^3J 5.6, J(^{195}Pt) 36.5, H^6), 7.91 (2H, t, ^3J 7.5, H^4), 7.69 (2H, d, ^3J 7.5, H^3), 7.51 (2H, s, H$^{3'}$), 7.46 (2H, d, ^3J 8.5, H^b), 7.23 (2H, t, ^3J 6.5, H^5), 6.74 (2H, d, ^3J 8.5, H^a), 3.81 (4H, t, ^3J 6.0, H$^\beta$), 3.71 (8H, m, H$^{\gamma,\varepsilon}$), 3.67 (8H, m, H$^{\alpha,\delta}$). ^{13}C NMR (126 MHz, $CDCl_3$): δ 167.5, 159.7, 152.3, 147.0, 141.2, 139.1 (C^4), 137.0, 129.1, 127.8 (C^b), 123.2 (C^5), 122.6 (C$^{3'}$), 119.4 (C^3), 111.9 (C^a), 71.5, 70.4, 70.3, 68.7 (C$^\beta$), 52.7 (C$^\alpha$). MS (ES$^+$): *m*/*z* 778.2 [M + Na$^+$], 719.4 [M–Cl]$^+$. HRMS (ES$^+$): 777.17832 [M + Na]$^+$; [$C_{32}H_{34}N_3O_4PtCl^{23}$Na] requires 777.17778.

PtL^{13}Cl From HL[13] (48 mg, 0.14 mmol) giving a bright yellow solid (55 mg, 72%). ^{1}H NMR (500 MHz, $CDCl_3$): δ 9.33 (2H, d, ^3J 5.5, $J(^{195}$Pt) 40, H^6), 7.94 (2H, t, ^3J 8.0, H^4), 7.73 (2H, d, ^3J 7.5, H^3), 7.56 (2H, s, H$^{3'}$), 7.55 (2H, m, H^b), 7.27 (2H, t, ^3J 6.0, H^5), 7.07 (2H, d, ^3J 8.0, H^a), 3.88 (3H, s, CH_3). ^{13}C NMR (126 MHz, $CDCl_3$): δ 167.4, 160.2, 159.2, 152.5 (C^6), 141.3, 139.2 (C^4), 136.7, 134.5, 128.1 (C^b), 123.4 (C^5), 123.2 (C$^{3'}$), 119.5 (C^3), 114.5 (C^a), 55.6 (CH_3). Anal. Calcd. for $C_{23}H_{17}N_2OPtCl.1/4CH_2Cl_2$: C 47.4, H 3.0, N 4.8%. Found: C 47.9, H 2.9, N 4.8%.

PtL^{14}Cl From HL[14] (64 mg, 0.17 mmol) giving a yellow solid (64 mg, 65%). ^{1}H NMR (500 MHz, $CDCl_3$): δ 9.28 (2H, d, ^3J 5.5, $J(^{195}$Pt) 40, H^6), 7.92 (2H, td, ^3J 7.5, ^4J 1.0, H^4), 7.72 (2H, d, ^3J 8.0, H^3), 7.52 (2H, s, H$^{3'}$), 7.23 (2H, ddd, ^3J 7.0, ^3J 6.0, ^4J 1.0, H^5), 7.16 (2H, m, H^b, H^d), 6.97 (1H, d, ^3J 8.7, H^a), 4.01 (3H, s, *m*-CH_3), 3.96 (3H, s, *p*-CH_3). ^{13}C NMR (126 MHz, $CDCl_3$): δ 167.2, 160.4, 152.4 (C^6), 149.5, 148.7, 141.2, 139.1 (C^4), 136.8, 135.0, 123.3 (C^5), 123.3 (C$^{3'}$), 119.5 (C^3), 119.4 (C^b), 111.7 (C^a), 110.5 (C^d), 56.4 (*m*-CH_3), 56.2 (*p*-CH_3). Anal. calcd for $C_{24}H_{19}N_2O_2PtCl.1/4CH_2Cl_2$: C, 45.3; H, 3.1; N, 4.3. Found: C, 45.1; H, 3.3; N, 4.2%.

PtL^{15}Cl From HL[15] (84 mg, 0.16 mmol) giving a yellow solid (33 mg, 28%). ^{1}H NMR (400 MHz, $CDCl_3$): δ 9.31 (2H, d, ^3J 5.7, $J(^{195}$Pt) 40, H^6), 7.94 (2H, td, ^3J 7.5, ^4J 1.5, H^4), 7.72 (2H, d, ^3J 8.0, H^3), 7.53 (2H, s, H$^{3'}$), 7.26 (2H, m, H^5), 7.16 (1H, s, H^d), 7.15 (1H, m, H^b), 6.97 (1H, d, ^3J 8.5, H^a), 4.29 (1H, t, ^3J 4.5, H$^{\alpha'}$), 4.23 (1H, t, ^3J 4.5, H$^\alpha$), 3.98 (2H, m, H$^\beta$, H$^{\beta'}$), 3.81 (2H, m, H$^\gamma$, H$^{\gamma'}$), 3.75 (2H, m, H$^\delta$, H$^{\delta'}$), 3.71 (2H, s, H$^\varepsilon$, H$^{\varepsilon'}$). MS (ES$^+$): *m*/*z* 794.2 [M + Na]$^+$, *m*/*z* 768.3 [M–Cl + MeOH]$^+$.

Electrochemical measurements

Cyclic voltammetry was carried out using a μAutolab Type III potentiostat with computer control and data storage *via* GPES Manager software. Solutions of concentration 1 mM in 90% CH_3CN/10% CH_2Cl_2 were used, containing [Bu_4N][BF_4] as the

supporting inert electrolyte. A three-electrode assembly was employed, consisting of a platinum working electrode, platinum wire counter electrode and platinum flag reference electrode. Solutions were purged for 5 minutes with solvent-saturated nitrogen gas with stirring, prior to measurements being taken without stirring. The voltammograms were referenced to a ferrocene-ferrocenium couple as the standard ($E^0 = 0.40$ *vs.* SCE).

Photophysical measurements

Absorption spectra were measured on a Biotek Instruments XS spectrometer, using quartz cuvettes of 1 cm path length. Steady-state luminescence spectra were measured using a Jobin Yvon FluoroMax-2 spectrofluorimeter, fitted with a red-sensitive Hamamatsu R928 photomultiplier tube; the spectra shown are corrected for the wavelength dependence of the detector, and the quoted emission maxima refer to the values after correction. Samples for emission measurements were contained within quartz cuvettes of 1 cm path length modified with appropriate glassware to allow connection to a high-vacuum line. Degassing was achieved *via* a minimum of three freeze-pump-thaw cycles whilst connected to the vacuum manifold; final vapour pressure at 77 K was $< 5 \times 10^{-2}$ mbar, as monitored using a Pirani gauge. Luminescence quantum yields were determined using quinine sulfate in 1M H_2SO_4 ($\phi = 0.546$[35]) and $[Ru(bpy)_3]Cl_2$ in air-equilibrated aqueous solution ($\phi = 0.028$[36]) as standards; estimated uncertainty in ϕ is ± 20% or better.

The luminescence lifetimes of the complexes were measured by time-correlated single-photon counting, following excitation at 374.0 nm with an EPL-375 pulsed-diode laser. The emitted light was detected at 90° using a Peltier-cooled R928 PMT after passage through a monochromator. The estimated uncertainty in the quoted lifetimes is ± 10% or better. Bimolecular rate constants for quenching by molecular oxygen, k_Q, were determined from the lifetimes in degassed and air-equilibrated solution, taking the concentration of oxygen in CH_2Cl_2 at 0.21 atm O_2 to be 2.2 mmol dm^{-3}.[37]

The quantum yields of singlet oxygen production were obtained by measuring the intensity of the $^1\Delta_g$ near-IR luminescence in an air-saturated solution in CH_2Cl_2, and comparing it with that measured for a solution of perinaphthenone {1-*H*-phenalen-1-one, $\Phi(^1O_2) = 0.95$[31]}. Solutions with optical density between 0.1 and 0.2 at 355 nm were used in each case. The samples were excited at 355 nm using the third harmonic of a Nd : YAG laser, and the emission in the near-IR was detected using a liquid-N_2-cooled germanium photodiode detector. A filter was used to eliminate light of < 1100 nm. Measurements at a range of incident light powers were made, and the quantum yields determined from the ratio of the gradients of intensity *vs.* power for the sample and standard, after correcting for any small differences between the absorbance of the sample and standard solutions at 355 nm. Representative plots are shown in the ESI†.

The instrumentation used in carrying out transient DC photoconductivity measurements is described in detail elsewhere.[25] A potential of 1000 V was used, applied over a gap of 0.25 mm; the orthogonal optical path length was 8 mm. The solution was degassed by purging with solvent-saturated argon, and the sample excited at 355 nm with the third harmonic of a Quantel Brilliant Nd : YAG laser (10 Hz, ~4 ns fwhm). Optical densities of around 1 were used at the excitation wavelength, and the absorption spectrum of the sample was verified after the measurements to ensure that no electrochemical degradation had occurred, induced by the field. Data was analysed by a global fitting procedure described previously,[38] based on that developed by Smirnov *et al.*[25]

Theory and calculations

The electronic structures were calculated by density functional theory (DFT) methods using the Gaussian 03[39] program package. Low-lying singlet and triplet excitation energies were calculated at optimized geometries by time-dependent DFT (TD-DFT). DFT calculations employed hybrid functionals; either B3LYP[40] or Perdew, Burke, Ernzerhof[41] (PBE0). The solvent was described by the polarizable conductor calculation model (CPCM).[42] Optimized excited-state geometry was calculated for the lowest triplet state by unrestricted Kohn–Sham (UKS) procedure. For H, C, N, O and Cl atoms, either polarized 6–31g* double – ζ basis sets[43] for geometry optimization and vibrational analysis, or cc-pvdz correlation consistent polarized valence double – ζ basis sets[44] (TD-DFT) were used, together with quasirelativistic effective core pseudopotentials and corresponding optimized set of basis functions for Pt.[45] The MO plots were drawn using the GaussView software. The spectral simulation was performed using the GaussSum software.[46] All calculated transitions are included. Gaussian shapes of the absorption bands are assumed. The fwhm value of 0.4 eV used corresponds to typical experimental bandwidths of MLCT bands.[47]

Acknowledgements

We thank EPSRC for support (grant ref. EP/D500265/1) and for a DTA studentship to D. L. R.; Frontier Scientific for supplying key starting materials; E.U. COST D35; and the Grant Agency of the Academy of Sciences of the Czech Republic (KAN100400702) and Ministry of Education of the Czech Republic (OC 139) for support to S. Z. We thank Prof. J. T. Hupp and Dr J. McGarrah for access to and assistance with instrumentation for TDCP. The authors are indebted to Drs S. Navaratnam and R. Edge for their assistance in measuring $^1O_2$ quantum yields, carried out with support from CCLRC Daresbury Laboratory, and to Dr J. A. Weinstein for discussions.

References

1 E. Polikarpov and M. E. Thompson, *Mater. Matters*, 2007, **2**(3), 21–23.
2 R. C. Evans, P. Douglas and C. Winscom, *Coord. Chem. Rev.*, 2006, **250**, 2093.
3 *Highly efficient OLEDs with phosphorescent materials*, ed. H. Yersin, Wiley-VCH, Weinheim, 2008.
4 S. Chakraborty, T. J. Wadas, H. Hester, R. Schmehl and R. Eisenberg, *Inorg. Chem.*, 2005, **44**, 6865.
5 J. R. Lakowicz, *Principles of Fluorescence Spectroscopy*, Springer, New York, 3rd edn, 2006, Chapters 20 and 22.
6 K. Suhling, P. M. W. French and D. Phillips, *Photochem. Photobiol. Sci.*, 2005, **4**, 13.
7 J. N. Demas and B. A. DeGraff, *Coord. Chem. Rev.*, 2001, **211**, 317.
8 For recent reviews, see for example: (*a*) D. R. McMillin and J. J. Moore, *Coord. Chem. Rev.*, 2002, **229**, 113; (*b*) S.-W. Lai and C.-M. Che, *Top. Curr. Chem.*, 2004, **241**, 27; (*c*) B. Ma, P. Djurovich and M. E. Thompson, *Coord. Chem. Rev.*, 2005, **249**, 1501; (*d*) F. N. Castellano, I. E. Pomestchenko, E. Shikhova, F. Hua, M. L. Muro and N. Rajapakse, *Coord. Chem. Rev.*, 2006, **250**, 1819; (*e*) K. M.-C. Wong

and V. W.-W. Yam, *Coord. Chem. Rev.*, 2007, **251**, 2477; (*f*) J. A. G. Williams, *Top. Curr. Chem.*, 2007, **281**, 205.
9 (*a*) For recent reviews of strategies for optimising the luminescence of Pt(II) complexes and applications in OLEDs: H.-F. Xiang, S.-W. Lai, P. T. Lai and C.-M. Che, *Phosphorescent platinum(II) materials for OLED applications*, in ref. 3; (*b*) J. A. G. Williams, S. Develay, D. L. Rochester and L. Murphy, *Coord. Chem. Rev.*, 2008, **252**, 2596.
10 (*a*) V. W.-W. Yam, K. M.-C. Wong and N. Zhu, *J. Am. Chem. Soc.*, 2002, **124**, 6506; (*b*) C. Yu, K. M.-C. Wong, K.H.-Y. Chan and V. W.-W. Yam, *Angew. Chem., Int. Ed.*, 2005, **44**, 791; (*c*) C.-M. Che, J.-L. Zhang and L.-R. Lin, *Chem. Commun.*, 2002, 2556; (*d*) C.-M. Che, W.-F. Fu, S.-W. Lai, Y.-J. Hou and Y.-L. Liu, *ibid.*, 2003, 118; (*e*) K. Wang, M. Haga, H. Monjushiro, M. Akiba and Y. Sasaki, *Inorg. Chem.*, 2000, **39**, 4022; (*f*) L. J. Grove, J. M. Rennekamp, H. Jude and W. B. Connick, *J. Am. Chem. Soc.*, 2004, **126**, 1594; (*g*) T. J. Wadas, Q. M. Wang, Y. J. Kim, C. Flaschenreim, T. N. Blanton and R. Eisenberg, *J. Am. Chem. Soc.*, 2004, **126**, 16841.
11 Recent examples include: (*a*) K.-H. Wong, M.C.-W. Chan and C.-M. Che, *Chem.–Eur. J.*, 1999, **5**, 2845; (*b*) V. W.-W. Yam, R. P.-L. Tang, K. M.-C. Wong, X.-X. Lu, K.-K. Cheung and N. Zhu, *Chem.–Eur. J.*, 2002, **8**, 4066; (*c*) P. K. M. Siu, S.-W. Lai, W. Lu, N. Zhu and C.-M. Che, *Eur. J. Inorg. Chem.*, 2003, 2749; (*d*) Q.-Z. Yang, Q.-X. Tong, L.-Z. Wu, L.-P. Zhang and C.-H. Tung, *Eur. J. Inorg. Chem.*, 2004, 1948; (*e*) W.-S. Tang, X.-X. Lu, K. M. C. Wong and V. W. W. Yam, *J. Mater. Chem.*, 2005, **15**, 2714; (*f*) H.-S. Lo, S.-K. Yip, K. M.- C. Wong, N. Zhu and V. W.-W. Yam, *Organometallics*, 2006, **25**, 3537.
12 J. A. G. Williams, A. Beeby, E. S. Davies, J. A. Weinstein and C. Wilson, *Inorg. Chem.*, 2003, **42**, 8609.
13 S. J. Farley, D. L. Rochester, A. L. Thompson, J. A. K. Howard and J. A. G. Williams, *Inorg. Chem.*, 2005, **44**, 9690.
14 W. Sotoyama, T. Satoh, N. Sawatari and H. Inoue, *Appl. Phys. Lett.*, 2005, **86**, 153505.
15 (*a*) M. Cocchi, D. Virgili, V. Fattori, D. L. Rochester and J. A. G. Williams, *Adv. Funct. Mater.*, 2007, **17**, 285; (*b*) J. Kalinowski, M. Cocchi, D. Virgili, V. Fattori and J. A. G. Williams, *Chem. Phys. Lett.*, 2006, **432**, 110; (*c*) D. Virgili, M. Cocchi, V. Fattori, C. Sabatini, J. Kalinowski and J. A. G. Williams, *Chem. Phys. Lett.*, 2006, **433**, 145.
16 (*a*) M. Cocchi, D. Virgili, V. Fattori, J. A. G. Williams and J. Kalinowski, *Appl. Phys. Lett.*, 2007, **90**, 023506; (*b*) M. Cocchi, J. Kalinowski, D. Virgili and J. A. G. Williams, *Appl. Phys. Lett.*, 2008, **92**, 113302.
17 (*a*) M. Cocchi, J. Kalinowski, D. Virgili, V. Fattori, S. Develay and J. A. G. Williams, *Appl. Phys. Lett.*, 2007, **90**, 163508; (*b*) J. Kalinowski, M. Cocchi, D. Virgili, V. Fattori and J. A. G. Williams, *Adv. Mater.*, 2007, **19**, 4000.
18 T. Ishiyama, M. Murata and N. Miyaura, *J. Org. Chem.*, 1995, **60**, 7508.
19 (*a*) C. J. Aspley and J. A. G. Williams, *New J. Chem.*, 2001, **25**, 1136; (*b*) W. Goodall, K. Wild, K. J. Arm and J. A. G. Williams, *J. Chem. Soc., Perkin Trans. 2*, 2002, 1669.
20 W. Sotoyama, T. Satoh, H. Sato, A. Matsuura and N. Sawatari, *J. Phys. Chem. A*, 2005, **109**, 9760.
21 Z. R. Grabowski, K. Rotkiewicz and W. Rettig, *Chem. Rev.*, 2003, **103**, 3899.
22 (*a*) C. J. Jödicke and H. P. Lüthi, *J. Am. Chem. Soc.*, 2003, **125**, 252; (*b*) D. Rappoport and F. Furche, *ibid.*, 2004, **126**, 1277; (*c*) K. A. Zachariasse, S. I. Druzhinin, W. Bosch and R. Machinek, *ibid.*, 2004, **126**, 1705; (*d*) A. Köhn and C. Hättig, *ibid.*, 2004, **127**, 7399; (*e*) J.-Y. Yang, K.-L. Liau, C.-M. Wang and C.-Y. Hwang, *ibid.*, 2004, **126**, 12325.
23 D. K. Crites, C. T. Cunningham and D. R. McMillin, *Inorg. Chim. Acta*, 1998, **273**, 346.
24 For a general review of Stark spectroscopy, see: (*a*) G. U. Bublitz and S. G. Boxer, *Annu. Rev. Phys. Chem.*, 1997, **48**, 213; (*b*) A review of Stark applied to inorganic systems: F. W. Vance, R. D. Williams and J. T. Hupp, *Int. Rev. Physc. Chem.*, 1998, **17**, 307.
25 S. N. Smirnov and C. L. Braun, *Rev. Sci. Instrum.*, 1998, **69**, 2875.
26 For a previous instance of the application of TDCP to a platinum(II) complex, see: F. W. M. Vanhelmont, R. C. Johnson and J. T. Hupp, *Inorg. Chem.*, 2000, **39**, 1814.
27 S. Goeb, A. A. Rachford and F. N. Castellano, *Chem. Commun.*, 2008, 814.
28 M. J. G. Peach, P. Benfield, T. Helgaker and D. J. Tozer, *J. Chem. Phys.*, 2008, **128**, 044118.
29 R. Y. Tsien, in *Fluorescent chemosensors for ion and molecule recognition*ed. A. W. Czarnik, ACS, Washington DC, 1992, pp. 130–146.
30 (*a*) Other recent examples of sensory systems employing the aryl-*N*-monoaza-15-crown-5 include ref.11d; (*b*) C.-T. Chen and W. P. Huang, *J. Am. Chem. Soc.*, 2002, **124**, 6246.
31 R. Schmidt, C. Tanielian, R. Dunsbach and C. Wolff, *J. Photochem. Photobiol., A*, 1994, **79**, 11.
32 J. N. Demas, E. W. Harris and R. P. McBride, *J. Am. Chem. Soc.*, 1977, **99**, 3547.
33 D. J. Cárdenas, A. M. Echavarren and M. C. Ramírez de Arellano, *Organometallics*, 1999, **18**, 3337.
34 W. Goodall and J. A. G. Williams, *Chem. Commun.*, 2001, 2514.
35 S. R. Meech and D. Phillips, *J. Photchem.*, 1983, **23**, 193.
36 K. Nakamaru, *Bull. Chem. Soc. Jpn.*, 1982, **55**, 2697.
37 S. L. Murov, I. Carmichael, and G. L. Hug, *Handbook of Photochemistry*, Marcel Dekker, New York, 2nd edn, 1993.
38 K. A. Waters, Y.-J. Kim and J. T. Hupp, *Inorg. Chem.*, 2002, **41**, 2909.
39 *Gaussian 03, Revision C.02*, M. J. Frisch, G. Trucks, H. B. Schlegel, G. E. Scuseria, M. A. Robb, J. R. Cheeseman, J. A. Montgomery, Jr., T. Vreven, K. N. Kudin, J. C. Burant, J. M. Millam, S. S. Iyengar, J. Tomasi, V. Barone, B. Mennucci, M. Cossi, G. Scalmani, N. Rega, G. A. Petersson, H. Nakatsuji, M. Hada, M. Ehara, K. Toyota, R. Fukuda, J. Hasegawa, M. Ishida, T. Nakajima, Y. Honda, O. Kitao, H. Nakai, M. Klene, X. Li, J. E. Knox, H. P. Hratchian, J. B. Cross, V. Bakken, C. Adamo, J. Jaramillo, R. Gomperts, R. E. Stratmann, O. Yazyev, A. J. Austin, R. Cammi, C. Pomelli, J. W. Ochterski, P. Y. Ayala, K. Morokuma, G. A. Voth, P. Salvador, J. J. Dannenberg, V. G. Zakrzewski, S. Dapprich, A. D. Daniels, M. C. Strain, O. Farkas, D. K. Malick, A. D. Rabuck, K. Raghavachari, J. B. Foresman, J. V. Ortiz, Q. Cui, A. G. Baboul, S. Clifford, J. Cioslowski, B. B. Stefanov, G. Liu, A. Liashenko, P. Piskorz, I. Komaromi, R. L. Martin, D. J. Fox, T. Keith, M. A. Al-Laham, C. Y. Peng, A. Nanayakkara, M. Challacombe, P. M. W. Gill, B. Johnson, W. Chen, M. W. Wong, C. Gonzalez and J. A. Pople, Gaussian, Inc., Wallingford CT, 2004.
40 A. D. Becke, *J. Chem. Phys.*, 1993, **98**, 5648.
41 J. P. Perdew, K. Burke and M. Ernzerhof, *Phys. Rev. Lett.*, 1996, **77**, 3865.
42 M. Cossi, N. Rega, G. Scalmani and V. Barone, *J. Comput. Chem.*, 2003, **24**, 669.
43 P. C. Hariharan and J. A. Pople, *Theor. Chim. Acta*, 1973, **28**, 213.
44 D. E. Woon and T. H. Dunning, Jr., *J. Chem. Phys.*, 1995, **103**, 4572.
45 D. Andrae, U. Häussermann, M. Dolg, H. Stoll and H. Preuss, *Theor. Chim. Acta*, 1990, **77**, 123.
46 N. M. O'Boyle, A. L. Tenderholt and K. M. Langner, *J. Comput. Chem.*, 2008, **29**, 839.
47 J. E. Monat, J. H. Rodriguez and J. K. McCusker, *J. Phys. Chem. A*, 2002, **106**, 7399.